

JOURNAL OF ENERGY, MATERIALS, AND INSTRUMENTATION TECHNOLOGY

Journal Webpage https://jemit.fmipa.unila.ac.id/



Fabrication of Bioceramic Carbonated Hydroxyapatite-Chitosan Composite Scaffold Derived from River Snail Shells via Freeze-Drying for Bone Grafting Applications

Rosita Wati*, Vayza Deva Alnovera, Aldi Herbanu, Endah, Sekar Asri Tresnaningtyas, Muhammad Wildan Gifari, and Marsudi Siburian

Department of Biomedical Engineering, Faculty of Industrial Technology, Institut Teknologi Sumatera, Lampung, Indonesia, 35365

Article Information

Article history: Received September 19, 2025 Received in revised form October 15, 2025 Accepted November 16, 2025

Keywords: bone tissue engineering, carbonated hydroxyapatite, chitosan, freeze-drying, scaffold

Abstract

The prevalence of bone fractures in Indonesia has increased by up to 8.5%, making cost-effective biomaterial alternatives for bone grafting applications necessary. This study aims to synthesize a hydroxyapatite carbonate (CHAp) composite scaffold from river snail shells (Semisulcospira libertina) and chitosan via freeze drying for bone tissue engineering applications. The shells were calcined at 1000°C to produce CaO, which was then synthesized into CHAp via a precipitation method with a Ca:P:CO3 molar ratio of 1.67:1:1. The CHAp/chitosan scaffold was fabricated at a 2:1 (w/w) ratio using freeze drying at -80°C for 72 hours. Characterization was performed using XRD, FTIR, SEM-EDX, and mechanical and degradation testing. XRD results showed that CHAp formed according to the JCPDS No. 09-0432 standard, exhibiting 85.61% crystallinity, a crystal size of 17.07 nm, and type B carbonate substitution. FTIR spectra confirmed the presence of PO43-, CO32-, and OH- groups. SEM-EDX analysis revealed a Ca/P ratio of 1.74 and a carbonate content of 4.06%. The scaffold has a porous structure with pore sizes ranging from 3.6 to 14 μ m. It has a compressive strength of 0.255 MPa, a maximum strain of 70.71%, and a gradual degradation profile reaching 40.79% in 48 hours. These results demonstrate that the CHAp/chitosan scaffold fabricated from river snail shells has physicochemical and mechanical properties suitable for bone grafting applications. This material offers a sustainable, cost-effective alternative for bone tissue regeneration.

Informasi Artikel

Proses artikel: Diterima 19 September 2025 Diterima dan direvisi dari 15 Oktober 2025 Accepted 16 November 2025

Kata kunci: bone tissue engineering, freeze-drying, karbonat hidroksiapatit, kitosan, scaffold

Abstrak

Kasus patah tulang di Indonesia menunjukkan peningkatan prevalensi mencapai 8,5% yang membutuhkan alternatif biomaterial cost-effective untuk aplikasi bone grafting. Penelitian ini bertujuan mensintesis scaffold komposit karbonat hidroksiapatit (CHAp) dari cangkang keong air sungai (Semisulcospira libertina) dengan kitosan menggunakan metode freeze-drying untuk aplikasi rekayasa jaringan tulang. Cangkang keong dikalsinasi pada 1000°C untuk menghasilkan CaO, kemudian disintesis menjadi CHAp melalui metode presipitasi dengan rasio molar Ca:P:CO3 = 1,67:1:1. Scaffold CHAp/kitosan difabrikasi dengan rasio 2:1 (w/w) menggunakan teknik freeze-drying pada -80°C selama 72 jam. Karakterisasi dilakukan menggunakan XRD, FTIR, SEM-EDX, uji mekanik, dan uji degradasi. Hasil XRD menunjukkan CHAp terbentuk sesuai standar JCPDS No. 09-0432 dengan kristalinitas 85,61%, ukuran kristal 17,07 nm, dan substitusi karbonat tipe B. Spektra FTIR mengkonfirmasi keberadaan gugus PO₄³-, CO₃²-, dan OH-. Analisis SEM-EDX menunjukkan rasio Ca/P sebesar 1,74 dengan kandungan karbonat 4,06%. Scaffold CHAp/kitosan memiliki struktur berpori dengan ukuran pori 3,6-14 µm, kuat tekan 0,255 MPa, regangan maksimum 70,71%, dan profil degradasi bertahap mencapai 40,79% dalam 48 jam. Hasil penelitian menunjukkan scaffold CHAp/kitosan dari cangkang keong air sungai berhasil difabrikasi dengan karakteristik fisikokimia dan mekanik yang sesuai untuk aplikasi bone grafting, menawarkan alternatif biomaterial berkelanjutan dan cost-effective untuk regenerasi jaringan tulang.

^{*} Corresponding author.

1. Introduction

Bone fracture cases in Indonesia show an alarming increase, with prevalence reaching 8.5% of the total population based on Riskesdas 2018, where traffic accidents contribute 31.4% of total cases (Kemenkes, 2018). Approximately 45% of cases occur in people over 60 years of age due to low-energy trauma related to osteoporosis (Rachman et al., 2023). High medical care costs and decreased productivity become major challenges for national health and economic systems (Rathod, 2020).

Conventional fracture treatment using metal implants such as titanium, stainless steel, and cobalt-chromium alloys is still constrained by high costs (Deveci et al., 2020), low biocompatibility, corrosion risk that triggers inflammation and local toxicity (Sukegawa et al., 2019), and stress shielding phenomena due to differences in elastic modulus that cause resorption and weakening of surrounding bone structures (Zhu et al., 2022). This condition encourages the development of more biocompatible and cost-effective biomaterial alternatives for bone grafting applications.

The development of tissue engineering and regenerative medicine has opened opportunities in developing synthetic scaffolds as a replacement for conventional bone grafts. Ideal scaffolds must meet criteria for biocompatibility, biodegradability, appropriate porosity, adequate mechanical properties, and osteoconductive ability that supports cell growth, vascularization, and new bone formation (Wong et al., 2023).

Hydroxyapatite (HAp) with formula Ca₁₀(PO₄)₆(OH)₂ becomes an alternative biomaterial because its chemical composition is very similar to natural bone minerals, which are composed of 70% HAp (Susanto, 2021). However, pure HAp has limitations because its stoichiometry is not completely identical to bone minerals, and its insoluble properties limit optimal bone regeneration ability (Susanto, 2021).

Carbonated hydroxyapatite (CHAp) with formula $Ca_{10-x}(PO_4)_{6-x}(CO_3)_x(OH)_{2-x-2y}(CO_3)_y$ was developed to overcome the limitations of pure HAp. CHAp has characteristics that more closely resemble natural bone mineral composition with carbonate content of 2-8% by weight (Sidiqa et al., 2020). Type-B CHAp, where CO_3^{2-} ions substitute PO_4^{3-} groups, most closely resembles biological apatite characteristics with low crystal energy, good stability, and high solubility that accelerates bone regeneration (Sidiqa et al., 2020).

Marine shells such as oyster (*Crassostrea gigas*), mussel (*Mytilus edulis*), and blood cockle (*Anadara granosa*) have been widely investigated as calcium sources for hydroxyapatite synthesis due to their high CaCO₃ content (95-98%) (Ram et al., 2023). However, marine shell-derived materials present significant challenges for biomedical applications. These shells require complex pre-treatment processes to remove organic impurities and often contain heavy metal contaminants (Cd, Pb, Hg) accumulated from marine pollution (Yap & Al-Mutairi, 2021). In Indonesia, marine shells from coastal areas face additional contamination risks from industrial waste, particularly in the Java Sea and Malacca Strait regions, where heavy shipping and manufacturing activities contribute to marine pollution (Yap & Al-Mutairi, 2021).

River snail shells (Semisulcospira libertina) have great potential as a natural calcium source with calcium carbonate content reaching more than 95% (Asimeng et al., 2020). This species is abundantly available in Indonesian freshwater ecosystems, particularly in aquaculture sites across Java, Sumatra, and Kalimantan, generating substantial shell waste that currently lacks valorization pathways. Unlike marine counterparts, river snail shells from freshwater sources exhibit lower heavy metal contamination due to minimal industrial pollutant exposure. The utilization of river snail shells addresses both biomaterial sustainability and environmental concerns related to aquaculture waste management, while providing a locally available, cost-effective calcium precursor for CHAp synthesis.

For optimal bone tissue engineering applications, CHAp needs to be combined with biodegradable polymers such as chitosan to form three-dimensional scaffolds. Chitosan, a natural polysaccharide from chitin deacetylation, has biodegradable, biocompatible, non-toxic properties, and a molecular structure similar to glycosaminoglycans (Mahanani et al., 2019). The combination of CHAp with chitosan is expected to produce composite scaffolds that combine the advantages of both materials: osteoconductive properties and high bioactivity from CHAp, as well as flexibility, cell adhesion ability, and antibacterial properties from chitosan.

The freeze-drying (lyophilization) method has proven effective in producing scaffolds with controlled porous structure, well-interconnected pores, and preservation of material bioactivity. This technique produces scaffolds with high porosity and controlled pore size that support cell infiltration, nutrient transport, and vascularization (Kamaruzaman et al., 2023). Controlled freezing processes enable ice crystal formation that can produce pores with an appropriate size and distribution for bone grafting applications (Song et al., 2024).

Based on the above description, this study aims to synthesize carbonated hydroxyapatite composite scaffolds from river snail shells (Semisulcospira libertina) with chitosan using the freeze-drying method and characterize their physicochemical and mechanical properties for bone grafting applications. This research is expected to produce biocompatible, cost-effective, and sustainable scaffold biomaterials as innovative alternatives in bone defect treatment.

2. Research Methods

2.1 Materials and Equipment

Materials used include river snail shells (Semisulcospira libertina) as CHAp source, acetone (Merck, pro analysis), chitosan (Merck, standard grade), diammonium hydrogen phosphate (DAP, (NH₄)₂HPO₄) (Merck), ammonium bicarbonate (NH₄HCO₃), deionized water, ammonium hydroxide (NH₄OH) 25% (Merck), and Phosphate Buffered Saline (PBS).

Equipment used includes a furnace, freeze dryer, magnetic stirrer with hot plate, pH meter, analytical balance, ball mill, mesh 150 and 170 sieves, burette, centrifuge, conical tube, and characterization equipment (SEM-EDX, XRD, FTIR, Universal Testing Machine).

2.2 Material Preparation

River snail shells were cleaned with running water and soft brushes, then soaked in acetone solution for 2×24 hours to remove protein residues (**Figure 1**). After drying for one day, the shells were dried in an oven at 100° C for 4 hours. Dried shells were ground using a ball mill and sieved with a mesh $150 (106 \mu m)$ to obtain a uniform particle size. Powder was then calcined at 1000° C for 4 hours to convert CaCO₃ to CaO through thermal decomposition (Lenz et al., 2020).

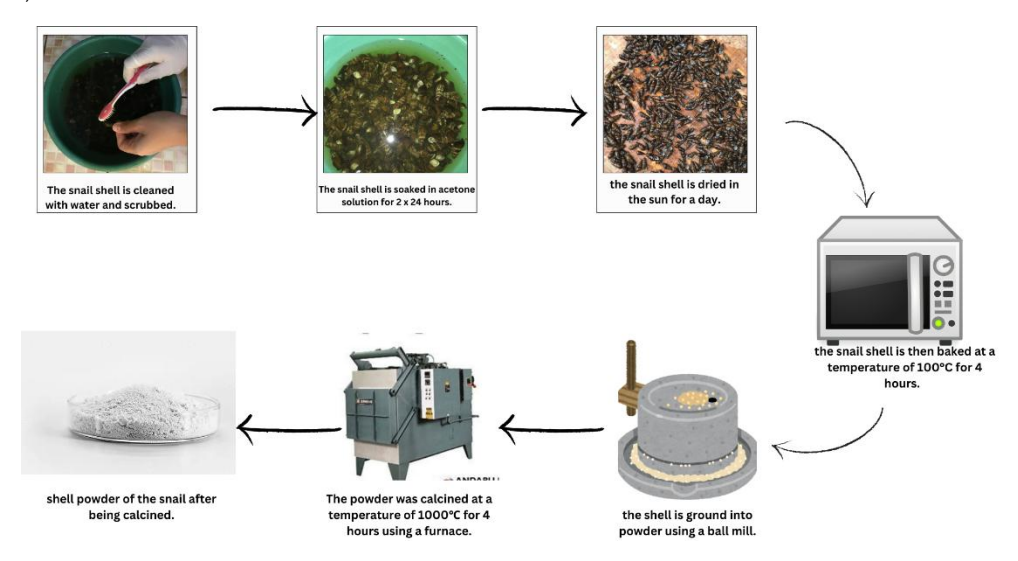


Figure 1. Material Preparation

2.3 Carbonated Hydroxyapatite (CHAp) Synthesis

CHAp was synthesized using the precipitation method with a Ca:P:CO $_3$ molar ratio = 1.67:1:1. 18.144 g CaO was dissolved in 210 mL of distilled water and stirred at 300 rpm for 1 hour at room temperature (**Figure 2**). The phosphate source was prepared by dissolving 25.662 g DAP in 210 mL of distilled water, then the pH was adjusted to \geq 10 with the addition of 27 mL NH $_4$ OH. The carbonate source was made by dissolving 15.357 g NH $_4$ HCO $_3$ in 105 mL of distilled water.

The mixing process was carried out by dropping carbonate solution into phosphate solution at a rate of 1 mL/minute while stirring at 300 rpm. The phosphate-carbonate mixture was then dropped into the calcium solution at the same rate. After mixing, the solution was stirred at 60°C for 1 hour, continued for 24 hours at room temperature, and then aged for 24 hours. Synthesis results were filtered, washed with distilled water, and centrifuged twice at 4000 rpm for 10 minutes. Precipitate was dried in a 90°C oven for 24 hours, ground with a mortar, sieved with a mesh 170, and sintered at 600°C for 2 hours to produce CHAp (Sawada & Nakano, 2022).

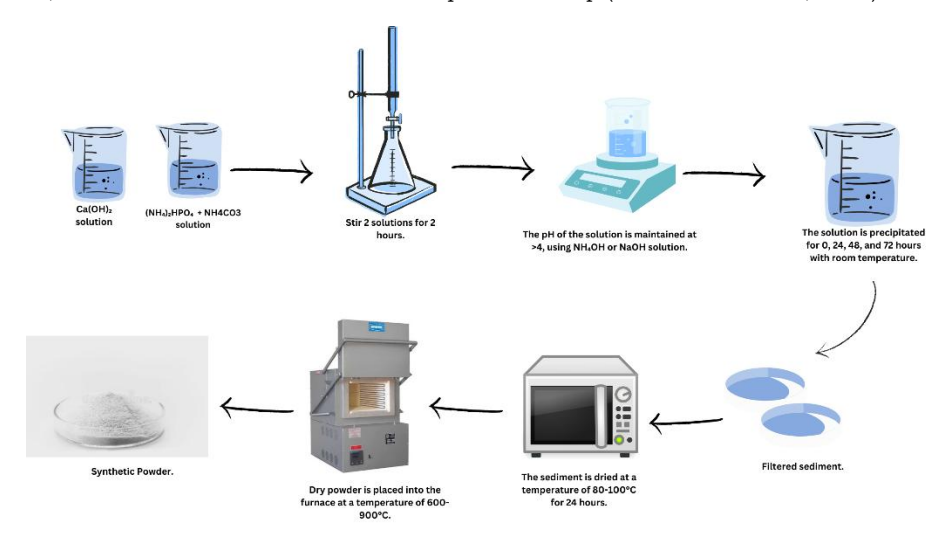


Figure 2. Stages of CHAp Synthesis

2.4 CHAp/Chitosan Scaffold Fabrication

Two grams of chitosan were dissolved in 100 mL of 2% acetic acid at room temperature with constant stirring. Separately, 4 g CHAp was dispersed in 50 mL of deionized water using ultrasonication. CHAp suspension was slowly

added to chitosan solution with CHAp: chitosan = 2:1 (w/w) ratio while stirring for 2-3 hours. pH of mixture was adjusted to 7.4 using 1M NaOH (10-15 mL) (Figure 3).

Homogeneous mixture was poured into low-temperature resistant molds, frozen at -80°C for a minimum of 72 hours, then freeze-dried for 24-48 hours under vacuum conditions with -80°C to -90°C condenser to produce porous scaffold structure (Sari et al., 2021).

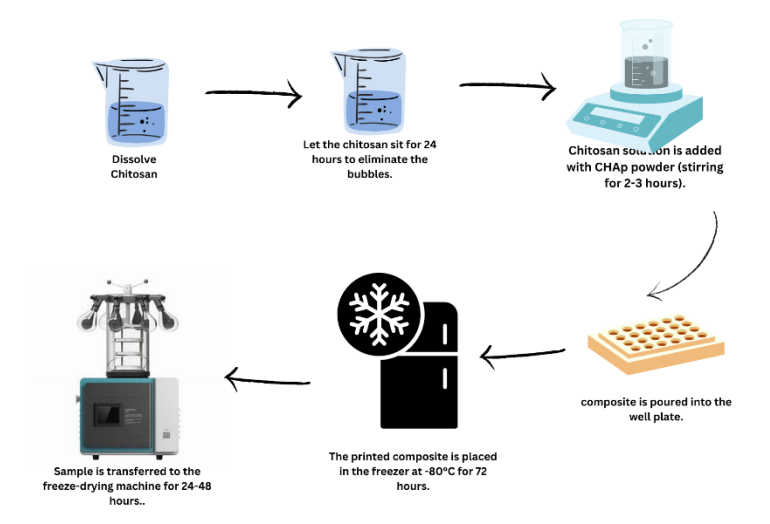


Figure 3. Fabrication stages of scaffold CHAp/CS.

2.5 Characterization

Crystal phase analysis using an X-ray diffractometer with JCPDS No. 09-0432 database for CHAp and JCPDS No. 37-1497 for CaO. Crystallinity calculation using the Scherrer equation. Functional group identification of PO_4^{3-} , CO_3^{2-} , and OH^- using an infrared spectrometer for type B carbonate substitution confirmation. Surface morphology and elemental composition using an electron microscope with Ca/P ratio and carbonate content analysis. Mechanical properties of the scaffold were determined using a Universal Testing Machine to determine compressive strength and maximum strain. Weight loss in PBS pH 7.4 at 37°C for 48 hours for scaffold stability and degradation profile evaluation (Permatasari et al., 2021).

3. Results and Discussions

3.1 CaO Powder Characterization from River Snail Shells

X-ray diffraction (XRD) analysis showed good formation of the calcium oxide (CaO) phase, as confirmed by diffraction patterns matching the JCPDS 37-1497 database. The XRD spectrum shows sharp characteristic CaO peaks with high intensity, indicating a good crystallinity level (**Figure 4**).

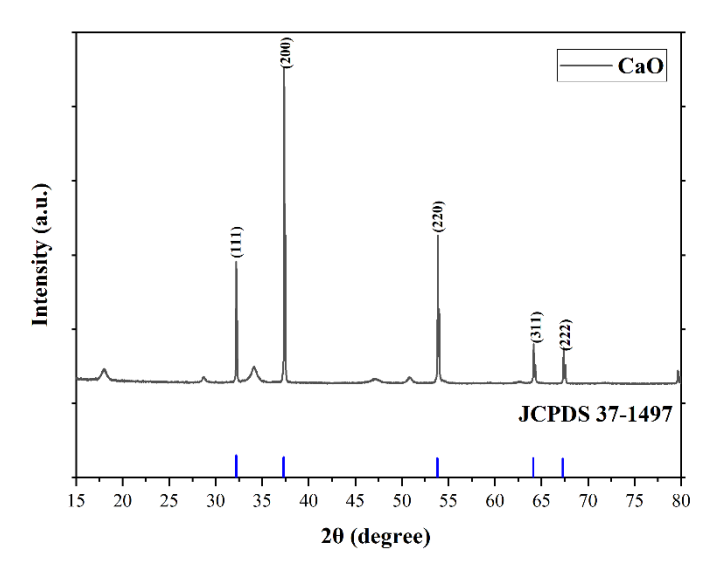


Figure 4. CaO diffraction pattern from river snail shells

Diffraction peaks obtained at 2θ positions = 32.2° (111), 37.3° (200), 53.8° (220), 64.1° (311), and 67.3° (222) show excellent agreement with JCPDS No. 37-1497 database. Main CaO diffraction peak identified at 2θ position = 37.3° corresponding to crystal plane (200), which is the most intense peak in CaO crystal structure according to findings (Weldeslase et al., 2023). High peak intensity and relatively narrow peak width indicate that the CaO sample has a fairly large crystal size and a high crystallinity level (Habte et al., 2019).

Analysis results show the presence of low intensity peaks from $Ca(OH)_2$ (at $2\theta = 18.0^{\circ}$) and $CaCO_3$ (at $2\theta = 28.6^{\circ}$) impurity phases. The presence of these impurity phases is likely due to hydration and carbonation processes occurring during sample storage in open air. Relatively low peak intensity indicates that the calcination process has proceeded well and the sample purity level is still acceptable (Daud et al., 2021). These results are supported by research by Inbaraj et al. (2023), showing that CaO from biological waste calcination produces particles with a pure poly-crystalline structure and a nanometer size.

3.2 CHAp Characterization from River Snail Shells

Crystal structure characterization of CHAp samples using X-ray diffraction (XRD) technique with diffractogram pattern analysis matched with JCPDS No. 09-0432 database, **Figure 5**. The most intense main diffraction peak was observed at an angle of around 31.8° corresponding to the crystal plane (211), followed by other characteristic peaks at plane (002) around 25.9°, plane (112) at 32.2°, plane (300) at 34.0°, and plane (202) at 34.7°.

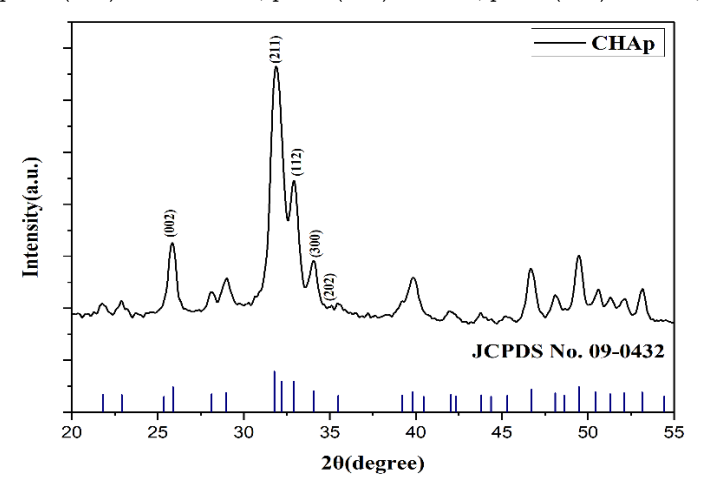


Figure 5. CHAp diffraction pattern from river snail shells

Comparison with JCPDS No. 09-0432 reference data shows peak position agreement with slight shifts on some reflection planes (**Table 1**). Peak shifts to higher 2 θ angles, especially at (300) and (202) peaks, indicate lattice parameter contraction due to carbonate substitution in hydroxyapatite structure (Safarzadeh et al., 2020).

Parameter	This study (River snail shell–derived CHAp)	Wati & Yusuf (2019) – Cockle shell–derived CHAp
Crystallinity (%)	85.61	Increased with sintering (not specified)
a (Å)	9.1242	9.422 (at 800 °C)
c (Å)	6.8700	6.895 (at 800 °C)
c∕a ratio	0.7529	1.366
Crystal size (nm)	17.07	30.6-61.2
Microstrain (ε)	0.00173	0.002-0.004

Table 1. Crystallographic parameters of CHAp from river snail shells

The XRD pattern of carbonated hydroxyapatite (CHAp) synthesized from river snail shells exhibited characteristic peaks corresponding to hydroxyapatite (HAp) at $20 \approx 31.7^{\circ}$, 32.2° , and 32.9° , which are assigned to the (211), (112), and (300) planes, respectively. These peaks are consistent with the standard HAp diffraction pattern (JCPDS No. 09-0432), indicating a single-phase apatite structure without secondary phases. Quantitative analysis revealed a crystallinity degree of 85.61% and an average crystallite size of 17.07 nm (Kawsar et al., 2024). The calculated lattice parameters were a = b = 9.1242 Å and c = 6.8700 Å, both slightly smaller than those of stoichiometric HAp from the JCPDS standard. The c/a ratio of 0.7529 lies within the characteristic range of 0.745–0.760, confirming the presence of B-type carbonate substitution in which CO_3^{2-} ions replace PO_4^{3-} groups (Copete et al., 2024; Kawsar et al., 2024). This carbonate incorporation typically causes a slight contraction of the a-axis and enhances solubility and bioactivity, consistent with previous findings for B-type CHAp synthesized from biogenic calcium sources.

When compared to the CHAp derived from cockle shells ($Cerastoderma\ edule$) reported by Rosita Wati and Yusril Yusuf (2019), which exhibited lattice parameters of a = 9.42 Å and c = 6.90 Å with crystallite sizes ranging from 30–61 nm (depending on sintering temperature), the CHAp from river snail shells showed slightly smaller lattice constants and finer crystallite dimensions. These findings suggest that the river snail shell–derived CHAp possesses a more compact lattice structure and lower microstrain (0.00173), indicating higher structural stability. The smaller

crystallite size also confirms the formation of nanoscale apatite crystals, which may enhance biological reactivity. Therefore, river snail shells represent a promising alternative biogenic calcium source capable of producing CHAp with a refined crystal structure and comparable or superior quality to other natural precursors (Wati & Yusuf, 2019).

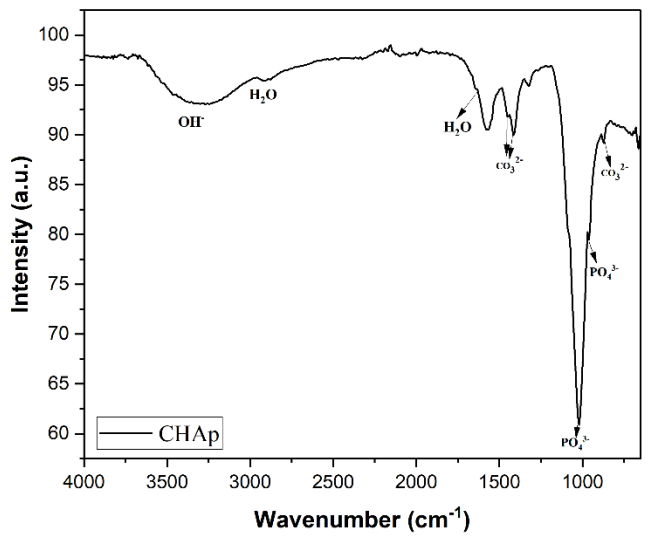


Figure 6. FTIR spectra of CHAp from river snail shells

FTIR analysis confirms successful carbonated hydroxyapatite synthesis **Figure 6**. The band at 3570.789 cm⁻¹ originates from the OH⁻ group stretching vibration. Carbonate (CO_3^{2-}) bands clearly observed at 1456.922 cm⁻¹, 1416.73 cm⁻¹ (stretching vibration) and 869.84 cm⁻¹ (bending vibration), indicating type B substitution. Phosphate (PO_4^{3-}) groups identified through bands at 1024.869 cm⁻¹, 966.0186 cm⁻¹, and bending bands at 602.86 cm⁻¹ and 564.1089 cm⁻¹ (Muarif et al., 2024).

CHAp morphology characterization shows irregularly shaped chunks with uneven surfaces due to irregular small particles adhering **Figure 7**. This morphology reflects the transformation of natural calcium carbonate structure to apatite structure through the sintering process.

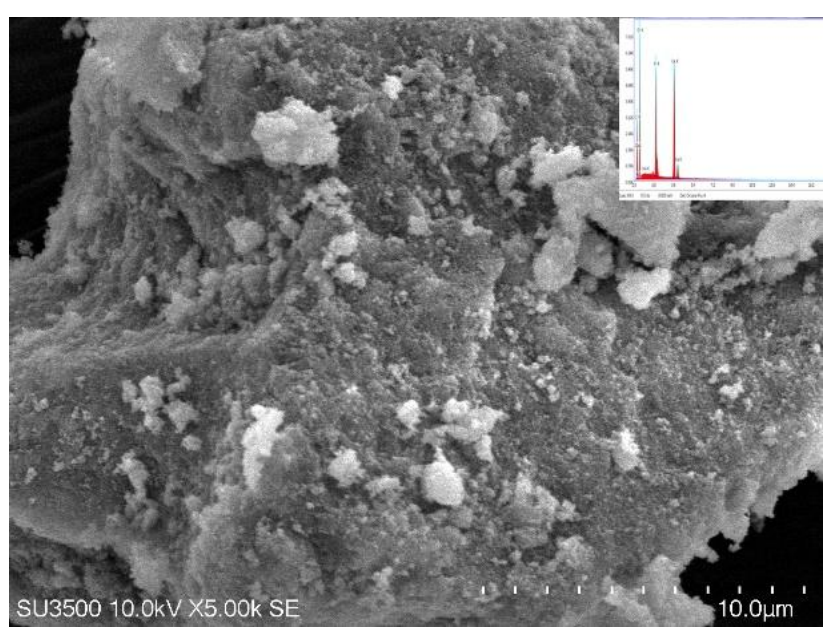


Figure 7. Morphology and EDX of CHAp from river snail shells

The Ca/P ratio of 1.74 is within an acceptable range for bioceramic materials, although slightly higher than the stoichiometric pure hydroxyapatite ratio (1.67). This value is supported by research by Jaffri et al. (2022), reporting similar Ca/P ratios in natural hydroxyapatite. Carbonate content of 4.06% confirms CO_3^{2-} ion substitution into the crystal structure through type B substitution.

3.3 CHAp/Chitosan Scaffold Characterization

Crystal structure characterization of CHAp/chitosan samples shows main peaks matching standard hydroxyapatite data Figure 8. In CHAp/chitosan, the intensity of (300) and (200) peaks increased compared to pure CHAp, indicating better crystal regularity after chitosan addition (Fihri et al., 2017).

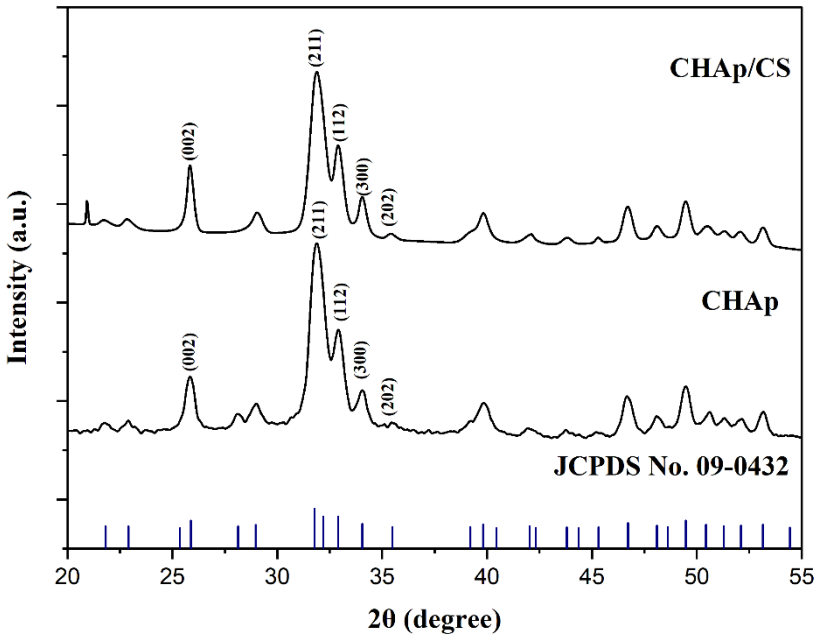


Figure 8. CHAp/CS diffraction pattern from river snail shells

Crystallinity increased from 85.61% in pure CHAp to 89.28% in CHAp/chitosan, showing chitosan's role in optimizing CHAp crystal growth. Microstrain value increased to 0.0066, indicating greater internal stress due to chitosan interactions (Habiburrohman et al., 2025).

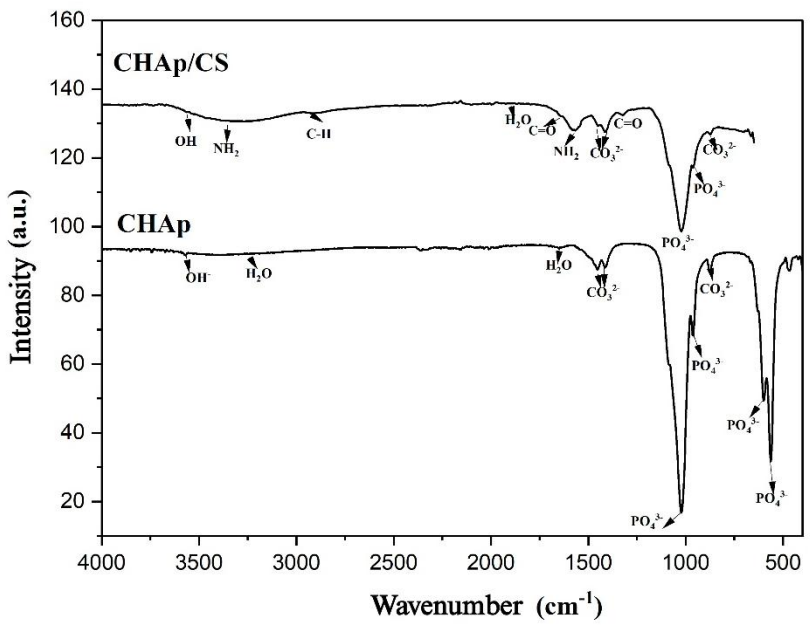


Figure 9. FTIR spectra of CHAp/chitosan from river snail shells

CHAp/chitosan composite shows significant changes compared to pure CHAp (**Figure 9**). PO_4^{3-} bands shifted, indicating interactions between phosphate groups from CHAp with chitosan functional groups. Appearance of new bands at 3347.15 cm⁻¹ (OH/NH stretching), 1572.93 cm⁻¹ (N-H bending), and 1647.49 cm⁻¹ (amide I) confirms chitosan presence in the composite (Said et al., 2021).

CHAp/chitosan scaffold morphology characterization using SEM reveals complex microstructure with formation of various-sized pores between 3.6-14 µm **Figure 10**. The formed porous structure provides a high specific surface area, advantageous for mass transport and cell adhesion.

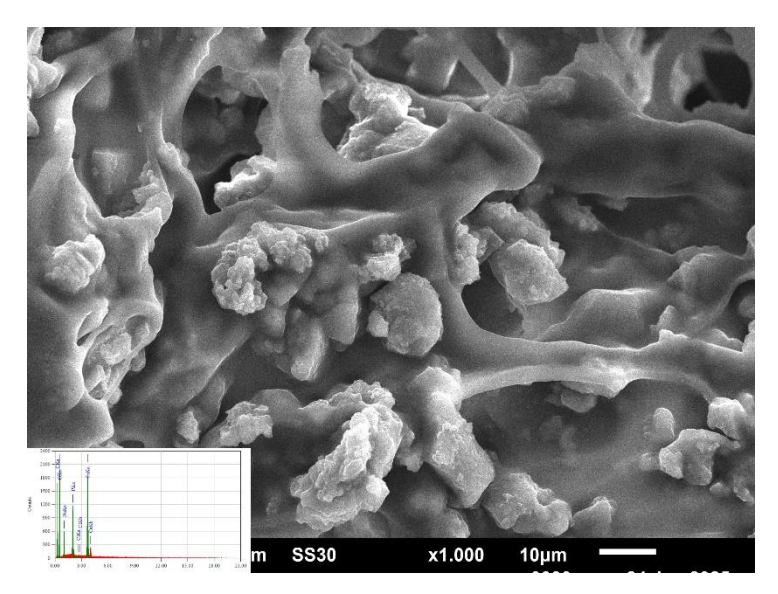


Figure 10. Morphology and EDX results of CHAp/chitosan

EDX analysis shows Ca/P ratio of 1.74, which is consistent. Carbonate content decreased to 2.63 wt% in the scaffold, possibly due to interactions with chitosan. A consistent Ca/P ratio indicates a suitable mineral composition for bone tissue engineering applications (Jaffri et al., 2022; Muarif et al., 2024).

Compressive test results on CHAp-chitosan scaffolds with a 2:1 ratio show a maximum compressive strength of 0.255 MPa with a maximum strain of 70.71%. The 2:1 ratio provides an ideal combination between hydroxyapatite strength and chitosan flexibility (Feng et al., 2020).

Gage Compressive Compressive Gage Length. Specimen Strain at Diameter **Cross Section** Length Strength crosshead length (mm) compressive (mm) (mm^2) (MPa) (mm) (mm) strength (%) 11.3 0.254937 70.71 13.3 138.9291 11.3 11.3

Table 2. Scaffold mechanical properties test results.

Maximum strain of 70.71% shows elasticity exceeding the physiological strain of human trabecular bone (1.0-2.5%) (Morgan et al., 2018). Compressive strength values are within the range of porous polymer scaffolds (~0.15-0.3 MPa) for trabecular bone tissue regeneration applications (Chinnasami et al., 2023).

Compared to the study by Rianti et al. (2023) using chitosan–gelatin–carbonate hydroxyapatite (C–G:CHA) based on limestone, compressive strength values of 2.19–4.19 MPa were obtained at ratio variations of 20:80 to 40:60 (w/w). These values are higher than those obtained in this study. This difference is caused by several factors. First, the different calcium raw material sources, where this study uses river snail shells (Semisulcospira libertina), which have a more porous structure and higher organic content compared to limestone. Second, Rianti et al. added gelatin as an additional polymer material that can enhance matrix bonding strength and scaffold density. Third, based on data in **Table 2**, CHAp from snail shells has a smaller crystallite size (17.07 nm), which can increase bioactivity but reduce mechanical strength (Rianti et al., 2023).

Thus, although the compressive strength value of this study's scaffold is lower, the high elastic properties and compressive strength value within the range of porous polymer scaffolds demonstrate good potential for non-load-bearing bone tissue applications (Rianti et al., 2023). For further research, mechanical strength can be improved through optimization of the chitosan:CHAp ratio, addition of reinforcing polymers such as gelatin, or use of crosslinkers to strengthen the scaffold matrix bonding.

CHAp/chitosan scaffold degradation testing in PBS solution at 37° C for 48 hours shows a three-phase degradation pattern **Figure 10**. The initial phase (0-3 hours) shows rapid degradation up to $23.27 \pm 2.62\%$. Second phase (3-24 hours) experiences deceleration with 31.34% weight loss. The third phase (24-48 hours) shows increased degradation reaching $40.79 \pm 3.25\%$ (Bozorgi et al., 2021; Khodaverdi et al., 2025).

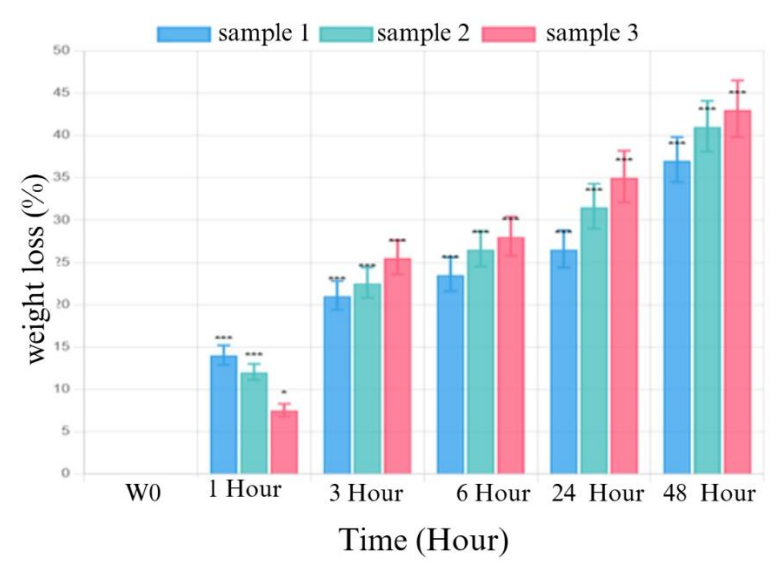


Figure 10. Degradation test results graph

A three-phase degradation profile has important implications for biomedical applications: the initial phase facilitates bioactive molecule release, the stabilization phase maintains structure for cell growth, and the advanced degradation phase enables tissue remodeling. Statistical analysis using one-way ANOVA shows highly significant differences (F = 35.490, p < 0.001), confirming the CHAp/chitosan scaffold has a controlled degradation profile for bone regeneration applications.

4. Conclusion

CHAp was successfully synthesized using the precipitation method from river snail shells with a crystal structure matching JCPDS No. 09-0432 standard and showing type B carbonate substitution in its crystal structure. Synthesized CHAp has physical and chemical characteristics supporting bioactivity with Ca/P ratio of 1.74, high crystallinity of 85.61%, and crystallite size of 17.07 nm. CHAp/chitosan scaffold was successfully fabricated using the freeze-drying method, producing a porous structure with pore sizes of 3.6-14 μ m and good material binding. CHAp/chitosan scaffold shows compressive strength of 0.255 MPa with high strain reaching 70.71%, and a gradual and controlled degradation profile, making it a potential candidate as a biomaterial for bone grafting and regenerative medicine applications.

5. Acknowledgement

The authors gratefully acknowledge the financial support from the Institute for Research and Community Service (LPPM), Institut Teknologi Sumatera (ITERA), under contract number 2658s/IT.9.2.1/PT.01.03/2025.

6. Bibliography

- Asimeng, B. O., Afeke, D. W., & Tiburu, E. K. (2020). Biomaterial for Bone and Dental Implants: Synthesis of B-Type Carbonated Hydroxyapatite from Biogenic Source. In *Biomaterials*. IntechOpen. https://doi.org/10.5772/intechopen.92256
- Bozorgi, A., Mozafari, M., Khazaei, M., Soleimani, M., & Jamalpoor, Z. (2021). Fabrication, characterization, and optimization of a novel copper-incorporated chitosan/gelatin-based scaffold for bone tissue engineering applications. *BioImpacts*. https://doi.org/10.34172/bi.2021.23451
- Chinnasami, H., Dey, M. K., & Devireddy, R. (2023). Three-Dimensional Scaffolds for Bone Tissue Engineering. *Bioengineering*, 10(7), 759. https://doi.org/10.3390/bioengineering10070759
- Copete, H., López, E., & Baudin, C. (2024). Synthesis and characterization of B-type carbonated hydroxyapatite materials: Effect of carbonate content on mechanical strength and in vitro degradation. *Boletín de La Sociedad Española de Cerámica y Vidrio*, 63(4), 255–267. https://doi.org/10.1016/j.bsecv.2023.12.001
- Daud, F. D. M., Azir, M. M. M., Mahmud, M. S., Sarifuddin, N., & Mohd Zaki, H. H. (2021). Preparation Of Cao-Based Pellet Using Rice Husk Ash Via Granulation Method For Potential CO2 Capture. *IIUM Engineering Journal*, 22(1), 234–244. https://doi.org/10.31436/iiumej.v22i1.1544
- Deveci, M. Z. Y., Gönenci, R., Canpolat, İ., & Kanat, Ö. (2020). In vivo biocompatibility and fracture healing of hydroxyapatite-hexagonal boron nitride- chitosan-collagen biocomposite coating in rats. *Turkish Journal of Veterinary And Animal Sciences*, 44(1), 76–88. https://doi.org/10.3906/vet-1906-21
- Feng, C., Zhang, K., He, R., Ding, G., Xia, M., Jin, X., & Xie, C. (2020). Additive manufacturing of hydroxyapatite bioceramic scaffolds: Dispersion, digital light processing, sintering, mechanical properties, and biocompatibility. *Journal of Advanced Ceramics*, 9(3), 360–373. https://doi.org/10.1007/s40145-020-0375-8

- Fihri, A., Len, C., Varma, R. S., & Solhy, A. (2017). Hydroxyapatite: A review of syntheses, structure, and applications in heterogeneous catalysis. *Coordination Chemistry Reviews*, 347, 48–76. https://doi.org/10.1016/j.ccr.2017.06.009
- Habiburrohman, M. R., Jamilludin, M. A., Cahyati, N., Herdianto, N., & Yusuf, Y. (2025). Fabrication and in vitro cytocompatibility evaluation of porous bone scaffold based on cuttlefish bone-derived nano-carbonated hydroxyapatite reinforced with polyethylene oxide/chitosan fibrous structure. *RSC Advances*, 15(7), 5135–5150. https://doi.org/10.1039/D4RA08457H
- Habte, L., Shiferaw, N., Mulatu, D., Thenepalli, T., Chilakala, R., & Ahn, J. (2019). Synthesis of Nano-Calcium Oxide from Waste Eggshell by Sol-Gel Method. Sustainability, 11(11), 3196. https://doi.org/10.3390/su11113196
- Inbaraj, S., Kannan, M., Boopathi, N. M., Soundararajan, R. P., & Rahale, C. S. (2023). Biological Preparation, Characterization of CaO Nanoparticles from Egg Shell Waste and Insecticidal Activity against Seed Weevil, Sitophilus oryzae L. in Maize. *International Journal of Environment and Climate Change*, 13(9), 2664–2671. https://doi.org/10.9734/ijecc/2023/v13i92497
- Jaffri, M. Z., Mohd Ismail, Z. M., Dermawan, S. K., & Abdullah, H. Z. (2022). Sample Preparation of the Natural Source Hydroxyapatite (HAp) derived from Black Tilapia Fish Scales. *Journal of Physics: Conference Series*, 2169(1), 012033. https://doi.org/10.1088/1742-6596/2169/1/012033
- Kamaruzaman, N., Fauzi, M. B., Tabata, Y., & Yusop, S. M. (2023). Functionalised Hybrid Collagen-Elastin for Acellular Cutaneous Substitute Applications. *Polymers*, 15(8), 1929. https://doi.org/10.3390/polym15081929
- Kawsar, M., Hossain, M. S., Bahadur, N. M., & Ahmed, S. (2024). Synthesis of nano-crystallite hydroxyapatites in different media and a comparative study for estimation of crystallite size using Scherrer method, Halder-Wagner method size-strain plot, and Williamson-Hall model. Heliyon, 10(3), e25347. https://doi.org/10.1016/j.heliyon.2024.e25347
- Kemenkes. (2018). Laporan Riskesdas 2018 Nasional.pdf. In Lembaga Penerbit Balitbangkes (p. hal 156).
- Khodaverdi, K., Naghib, S. M., Mozafari, M. R., & Rahmanian, M. (2025). Chitosan/hydroxyapatite hydrogels for localized drug delivery and tissue engineering: A review. *Carbohydrate Polymer Technologies and Applications*, 9, 100640. https://doi.org/10.1016/j.carpta.2024.100640
- Lenz, S., Dubois, N., Geist, J., & Raeder, U. (2020). Phacotus lenticularis content in carbonate sediments and epilimnion in four German hard water lakes. *Journal of Limnology*, 79(2), 187–197. https://doi.org/10.4081/jlimnol.2020.1945
- Mahanani, E. S., Khusnatunnisa, K., & Mutmainnah, M. (2019). Efektivitas Inkorporasi Platelet Rich Plasma pada Perancah Hidrogel CaCO3. Insisiva Dental Journal: Majalah Kedokteran Gigi Insisiva, 8(2). https://doi.org/10.18196/di.8206
- Morgan, E. F., Unnikrisnan, G. U., & Hussein, A. I. (2018). Bone Mechanical Properties in Healthy and Diseased States. *Annual Review of Biomedical Engineering*, 20(1), 119–143. https://doi.org/10.1146/annurev-bioeng-062117-121139
- Muarif, M. F., Yusuf, Y., & Agipa, A. I. (2024). Type-B Carbonated Hydroxyapatite Based on Crab Shells: A Review on Synthesis and Characterization. *Journal of Energy, Material, and Instrumentation Technology*, 5(1), 35–42. https://doi.org/10.23960/jemit.v5i1.241
- Permatasari, H. A., Sari, M., Aminatun, Suciati, T., Dahlan, K., & Yusuf, Y. (2021). Nano-carbonated hydroxyapatite precipitation from abalone shell (Haliotis asinina) waste as the bioceramics candidate for bone tissue engineering. Nanomaterials and Nanotechnology, 11, 184798042110328. https://doi.org/10.1177/18479804211032851
- Rachman, T., Rahmadian, R., & Rusjdi, S. R. (2023). Pola Penatalaksanaan Fraktur Femur Di RSUP Dr. M. Djamil Padang tahun 2020. *Jurnal Ilmu Kesehatan Indonesia*, 4(2), 81–87. https://doi.org/10.25077/jikesi.v4i2.624
- Ram, U. B., Sujatha, V., Vidhya, S., Jayasree, R., & Mahalaxmi, S. (2023). Oyster shell-derived nano-hydroxyapatite and proanthocyanidin pretreatment on dentinal tubule occlusion and permeability before and after acid challenge—an in vitro study. *Journal of Materials Science: Materials in Medicine*, 34(4), 17. https://doi.org/10.1007/s10856-023-06724-4
- Rathod, C. L., & Yadav, G. (2020). A Cross Sectional Study Of Clinico-Demographic Profile Of Patients With Complex Proximal Femoral Fractures. *International Journal of Medical and Biomedical Studies*, 4(8), 128–130. https://doi.org/10.32553/ijmbs.v4i8.1445
- Rianti, D., Purnamasari, A. E., Putri, R. R., Salsabilla, N. Z., Faradillah, Munadziroh, E., Agustantina, T. H., Meizarini, A., Yuliati, A., & Syahrom, A. (2023). The compressive strength and static biodegradation rate of chitosan-gelatin limestone-based carbonate hydroxyapatite composite scaffold. *Dental Journal*, 56(3), 160–165. https://doi.org/10.20473/j.djmkg.v56.i3.p160-165
- Safarzadeh, M., Ramesh, S., Tan, C. Y., Chandran, H., Ching, Y. C., Noor, A. F. M., Krishnasamy, S., & Teng, W. D. (2020). Sintering behaviour of carbonated hydroxyapatite prepared at different carbonate and phosphate ratios. Boletín de La Sociedad Española de Cerámica y Vidrio, 59(2), 73–80. https://doi.org/10.1016/j.bsecv.2019.08.001

- Said, H. A., Noukrati, H., Ben Youcef, H., Bayoussef, A., Oudadesse, H., & Barroug, A. (2021). Mechanical Behavior of Hydroxyapatite-Chitosan Composite: Effect of Processing Parameters. *Minerals*, 11(2), 213. https://doi.org/10.3390/min11020213
- Sari, M., Suciati, T., Dahlan, Ka., & Yusuf, Y. (2021). Nanostructure of carbonated hydroxyapatite precipitation extracted from pearl shells (Pinctada maxima) by pH treatment. 16(4), 1619–1625.
- Sawada, N., & Nakano, T. (2022). Insights into sex-related size and shape dimorphism in Semisulcospira niponica (Caenogastropoda: Cerithioidea: Semisulcospiridae). *Journal of Molluscan Studies*, 88(2). https://doi.org/10.1093/mollus/eyac013
- Sidiqa, A. N., Rahaju, A., Trilarasati, T., & Khoirunnisa, M. (2020). Pengukuran kekerasan karbonat apatit dengan penguat zirkonia sebagai aplikasi implan gigi Hardness evaluation of carbonate apatite reinforced with zirconia as a dental implant. *Padjadjaran Journal of Dental Researchers and Students*, 4(1), 21. https://doi.org/10.24198/pjdrs.v4i1.25710
- Song, X., Philpott, M. A., Best, S. M., & Cameron, R. E. (2024). Controlling the Architecture of Freeze-Dried Collagen Scaffolds with Ultrasound-Induced Nucleation. *Polymers*, 16(2), 213. https://doi.org/10.3390/polym16020213
- Sukegawa, S., Kanno, T., Yamamoto, N., Nakano, K., Takabatake, K., Kawai, H., Nagatsuka, H., & Furuki, Y. (2019).

 Biomechanical Loading Comparison between Titanium and Unsintered Hydroxyapatite/Poly-L-Lactide Plate
 System for Fixation of Mandibular Subcondylar Fractures. *Materials*, 12(9), 1557.
 https://doi.org/10.3390/ma12091557
- Susanto, R. (2021). Potensi Pembuatan Replika Tulang Berpori Menggunakan Template Ampas Tebu. CHEMPUBLISH JOURNAL, 5(2), 116–129. https://doi.org/10.22437/chp.v5i2.10612
- Wati, R., & Yusuf, Y. (2019). Effect of Sintering Temperature on Carbonated Hydroxyapatite Derived from Common Cockle Shells (Cerastodermaedule): Composition and Crystal Characteristics. Key Engineering Materials, 818, 37–43. https://doi.org/10.4028/www.scientific.net/KEM.818.37
- Weldeslase, M. G., Benti, N. E., Desta, M. A., & Mekonnen, Y. S. (2023). Maximizing biodiesel production from waste cooking oil with lime-based zinc-doped CaO using response surface methodology. *Scientific Reports*, 13(1), 4430. https://doi.org/10.1038/s41598-023-30961-w
- Wong, S. K., Yee, M. M. F., Chin, K.-Y., & Ima-Nirwana, S. (2023). A Review of the Application of Natural and Synthetic Scaffolds in Bone Regeneration. *Journal of Functional Biomaterials*, 14(5), 286. https://doi.org/10.3390/jfb14050286
- Yap, C. K., & Al-Mutairi, K. A. (2021). Ecological-Health Risk Assessments of Heavy Metals (Cu, Pb, and Zn) in Aquatic Sediments from the ASEAN-5 Emerging Developing Countries: A Review and Synthesis. *Biology*, 11(1), 7. https://doi.org/10.3390/biology11010007
- Zhu, Y., Shao, Y., Guan, T., Lin, B., Guo, C., & Pan, T. (2022). Analysis of the Stress between Implant Prostheses with Different Moduli and Surrounding Bones. https://doi.org/10.21203/rs.3.rs-1358844/v1